Available online at www.sciencedirect.com

ScienceDirect

journal homepage: www.elsevier.com/locate/he

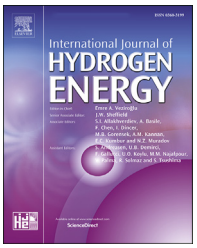

# Density functional theory calculations of iron - vanadium carbide interfaces and the effect of hydrogen

*Sebastián Echeverri Restrepo* [a,b,*], *Davide Di Stefano* [c], *Matous Mrovec* [d], *Anthony T. Paxton* [b]

[a] *SKF Research & Technology Development (RTD), SKF B.V., Meidoornkade 14, 3992 AE, Houten, the Netherlands*
[b] *Department of Physics, King's College London, Strand, London, WC2R 2LS, United Kingdom*
[c] *ANSYS Granta, Rustat House 62 Clifton Road Cambridge, CB1 7EG, United Kingdom*
[d] *ICAMS, Ruhr-Universität Bochum, D-44780, Bochum, Germany*

## HIGHLIGHTS

- A DFT study of H in perfect and defective Fe/VC interfaces was carried out.
- The perfect (100)Fe/(100)VC coherent interface traps H only weakly.
- C vacancies are deeper traps, both at the interface and in VC bulk.
- Thermodynamic estimates show a negligible influence of H on the interface strength.

## ARTICLE INFO

*Article history:*
Received 7 August 2019
Received in revised form
8 October 2019
Accepted 14 November 2019
Available online xxx

*Keywords:*
Hydrogen embrittlement
Interfaces
Density functional theory
Vanadium carbides

## ABSTRACT

According to recent experimental research, vanadium-carbide precipitates can improve hydrogen resistance and hardness in steels. In the present article, density functional theory calculations are performed to study the structure and energetics of iron–vanadium carbide interfaces and how hydrogen interacts with them. A comparison of the solubility of hydrogen in different sites shows that hydrogen will tend to segregate towards the iron –vanadium carbide interface and that carbon vacancies within a vanadium carbide precipitate behave as strong hydrogen traps. Additionally, it is shown that the presence of hydrogen at an iron–vanadium carbide interface does not cause a significant embrittlement of the material.



## Introduction

Bearing steels need to cope with severe cyclic and static loads, especially those generated by rolling contact fatigue. Usually the type of steels that better comply with all these requirements are those that are hardened via heat treatments to contain a martensitic or bainitic structure. They must also have high hardness, strength and toughness and, due to the varying working environmental conditions, they need to be resistant to corrosion and to the effects of hydrogen (H) [1].

* *Corresponding author*. SKF Research & Technology Development (RTD), SKF B.V., Meidoornkade 14, 3992 AE, Houten, the Netherlands.
E-mail address: sebastianecheverrir@gmail.com (S. Echeverri Restrepo).

https://doi.org/10.1016/j.ijhydene.2019.11.102
0360-3199/

In the case of bearing applications, H can penetrate the steel due to the decomposition of the lubricant, the presence of water in the lubricant, fretting and/or other corrosion reactions. There is ample evidence that support the fact that the presence of H in bearing steels leads to a degradation of its mechanical properties, including the resistance to fatigue regardless of the mode of loading [1–4].

Although there have been several mechanisms proposed to explain the way that H causes embrittlement on steels [5], in the case of bearings subjected to rolling contact fatigue, recent work presents strong evidence that H accelerates damage via the formation of white etching areas with associated cracks [6]. This supports the hypothesis that H-enhanced localised plasticity [7] is the principal H embrittlement mechanism in bearing steels [6].

The presence of transition metal carbides and nitrides can affect the distribution of H in the steel matrix as well as hydrogen diffusivity. It has been suggested that these particles may efficiently trap H and thus lower the steel's susceptibility to H embrittlement. For instance, a tailored precipitation of vanadium carbide (VC) particles was demonstrated to reduce the damage due to H embrittlement [8].

In the present work, H trapping at the interfaces between VC and Body-Centred-Cubic (BCC) Fe matrix using first-principles calculations based on Density Functional Theory (DFT) [9,10] is investigated. The aim is to determine whether these interfaces can act as efficient traps for the immobilisation of H, as has been seen in experiments [11–13] and in the TiC–Fe system [14]. Additionally, we calculate the solubility of H at the VC-Fe interface considering C-vacancies and we estimate the effect of segregated H on the cohesive strength of the interfaces via the theoretical work of separation.

The present article is divided into four parts. In the first part, the computational details are summarised; in the second part, the properties of individual phases are presented; in the third part, the structure and energetics of the clean interface is investigated; finally, in the fourth part, the behaviour of hydrogen at the interface is studied.

## Computational details

### *General simulation parameters*

All calculations were performed by means of density functional theory simulations [9,10] using the ABINIT code [15]. A Generalised Gradient Approximation (GGA) [16–19] in the form given by Perdew, Burke and Ernzerhof [20] was employed for the exchange-correlation and projector augmented wave (PAW) potentials [21–23] were used to describe the core electrons. For all the systems, total energy convergence tests in terms of the **k**-points, number of bands, temperature of smearing and cut-off energy were performed using a convergence limit of $4 \times 10^{-5}$ $E_h$/atom, where $E_h$ is the Hartree energy. For the supercells with and without H, both ionic positions and cell vectors were relaxed using $5 \times 10^{-5} E_h a_0^{-1}$ as convergence limit of the forces for structural optimisations, where $a_0 = 0.529$Å is the Bohr radius. All calculations were carried out as spin-polarised. Additional computational details, relative to each specific systems, can be found in Table 1.

## Individual phases

In order to be able to investigate the Fe-VC interface as well as the interaction with H, the fundamental properties of individual elemental phases were computed. The investigated systems are summarised in Table 1 together with the computational details used for the calculations.

For $H_2$, two H atoms were inserted in a cubic box of dimensions $13 \times 13 \times 13$ $a_0$. Since the system contains only a single $H_2$ molecule placed in a large simulation cell, only one **k**-point was used. After structural relaxation, the equilibrium interatomic distance for the $H_2$ molecule of 1.434 $a_0$ was obtained, in agreement with other values reported in the literature [24].

The structure of VC belongs to the space group $Fm\bar{3}m$, No. 225. The calculation of its lattice parameter is carried out using the primitive unit cell containing 1 V and 1C atoms. A simultaneous structural minimisation of the cell geometry and the position of the atoms using the Broyden-Fletcher-Goldfarb-Shanno minimisation (BFGS) as implemented in the software ABINIT was used to obtain the equilibrium structure. A lattice parameter of 4.155 Å was found, consistent with other experimental and theoretical values available in the literature (see Table 2).

A similar procedure was followed for BCC V using a cell containing one single atom (space group $Im\bar{3}m$, No. 229) and for C in its graphite structure (space group $P63mc$, No. 186). The

**Table 1 – Calculation details for the DFT calculations performed. The units for the smearing temperature and the cut-off energy are.$E_h$**

| | Calculation details | | | | |
|---|---|---|---|---|---|
| | **k**-point grid | **k**-points | Bands | Smearing temperature | Cut-off energy |
| $H_2$ | | 1 | 2 | 0.0015 | 14 |
| V | $18 \times 18 \times 18$ | 190 | 12 | 0.001 | 36 |
| C | $19 \times 19 \times 19$ | 400 | 32 | 0.001 | 36 |
| Fe | $6 \times 6 \times 6$ | 108 | 1156 | 0.0005 | 46 |
| VC | $9 \times 9 \times 9$ | 85 | 15 | 0.001 | 36 |
| $Fe_{surface}$ | $6 \times 6 \times 2$ | 36 | 450 | 0.0009 | 37 |
| $VC_{surface}$ | $6 \times 6 \times 2$ | 36 | 450 | 0.0009 | 37 |
| Fe – $VC_{interface}$ | $6 \times 6 \times 2$ | 36 | 450 | 0.0009 | 37 |

Please cite this article as: Echeverri Restrepo S et al., Density functional theory calculations of iron - vanadium carbide interfaces and the effect of hydrogen, International Journal of Hydrogen Energy, https://doi.org/10.1016/j.ijhydene.2019.11.102

**Table 2 – Calculated values of the lattice parameters for VC, V, C and Fe. Theoretical and experimental values from literature are presented for comparison when available. The units are [Å].**

| | Lattice Parameters | | |
|---|---|---|---|
| | Present work | Theory | Experiment |
| VC | 4.155 | 4.155 [25]; 4.174 [26]; 4.107 [26]; 4.156 [27] 4.164 [30]; 4.161 [31]; 4.160 [32]; 4.138 [29] 4.136 [33]; 4.095 [34]; 4.162 [34]; 4.129 [34] | 4.163 [28]; 4.169 [29] |
| V | 2.996 | 3.032 [35]; 2.990 [35]; 2.988 [35]; 2.926 [35] 2.999 [37] | 3.0399 [36] |
| C | 2.468, 8.704 | 2.461, ~9 [38]; 2.441, 6.664 [38]; 2.45, 6.6 [39] 2.47, ≫7.5 [39]; 2.47, 7.0 [39] | 2.456, 6.672 [40] |
| Fe | 2.836 | 2.833 [41]; 2.831 [42]; 2.835 [42]; 2.767 [43] 2.869 [43] | 2.853 [41]; 2.858 [44]; 2.855 [44]; 2.866 [45] |

calculated lattice parameters for V and C are 2.996 Å and 2.468 Å, 8.704 Å, respectively.

For Fe (ferrite), a cubic cell containing 16 atoms organised in a BCC structure was generated; this larger supercell was necessary for accurate determination of the H dissolution energy (see below). A structural minimisation of the system resulted in an equilibrium lattice parameter of 2.836 Å, consistent with other values found in the literature (see Table 2). In the case of other simulations of Fe containing H, the same simulation parameters were used as the ones shown in Table 1.

## The pristine interface

### *Structure*

The studied interface is formed between Fe(100) and VC(100) crystals in the so called Baker-Nutting orientation relationship, which is frequently observed experimentally for carbide precipitates with a B1 crystal structure (rocksalt) embedded in a ferrite matrix ($\alpha$) [2,11,46–48]. This misorientation is expressed as

$$(100)_{\alpha}\|(100)_{VC} \qquad [010]_{\alpha}\|[011]_{VC} \tag{1}$$

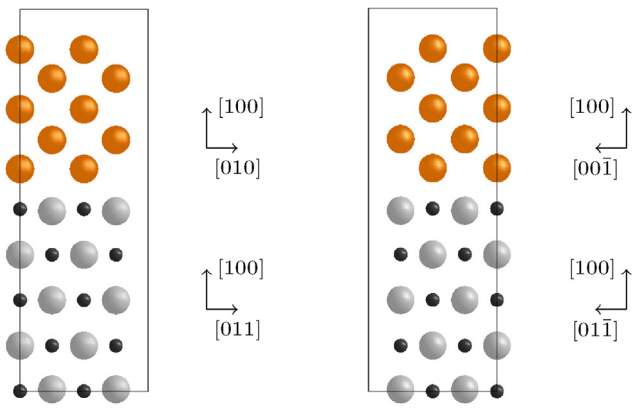


**Fig. 1 – Front and side view of the interface between Fe and VC. The system is composed of 20 Fe, 20 V and 20C atoms, drawn in orange, grey and black, respectively. (For interpretation of the references to colour in this figure legend, the reader is referred to the Web version of this article.)**

In this orientation relationship the different lattice parameters of the two phases lead to a lattice mismatch which, for precipitates larger than about 10 nm, is accommodated by misfit dislocations. Moreover experimental observations suggest that it is possible to have a predominantly coherent interface [8,13]. For these reasons only coherent interfaces were considered.

Additional to the relative misorientation of the grains, which define the five macroscopic degrees of freedom (DoFs) [49–51], three other microscopic DoFs that represent relative rigid translations of the grains need to be defined. In order to find the most stable interface, different possible rigid translations were tried. The most stable configuration results to be that with the Fe atoms positioned right on top of the C atoms.

The atomic structure of the investigated interface is shown in Fig. 1. The supercell contains of 5 Fe, and 5 VC atomic layers; previous studies have shown that a system of such size is sufficiently large for the accurate calculation of the interfacial energy and of the dissolution energy of H at a coherent interface [14,42,52].

After the generation of the interface, a simultaneous structural minimisation of the cell geometry and the position of the atoms was carried out. The resulting dimensions of the system along the plane of the interface per unit cell are 2.925 Å × 2.925 Å (for comparison, in Refs. [53,54] values of 2.909 Å and of 2.949 Å were found, respectively). This represents an expansion of the lattice parameter of Fe of 3% and a contraction of 0.5% for VC. As expected, the elastically softer Fe phase expands to match the lattice parameter of VC. All the calculations of the Fe-VC interface, including those containing H and/or C vacancies, were done using the parameters shown in Table 1.

The calculation of the free surfaces is conducted in a similar way, taking as a reference the system containing the interface. The size of the system is defined based on previous studies available in the literature where it has been shown that, for similar systems, the surface energy converges to within 0.05 J $m^{-2}$ for slabs with 5 or more layers of atoms [55].

In the case of VC, the Fe atoms are removed leaving a slab of 5 VC atom layers with two free surfaces. The dimensions of the simulation box along the interface plane and the atom positions are then modified in such a way that the previously calculated equilibrium bulk lattice parameter is respected. The size of the box perpendicular to the interface is not

Please cite this article as: Echeverri Restrepo S et al., Density functional theory calculations of iron - vanadium carbide interfaces and the effect of hydrogen, International Journal of Hydrogen Energy, https://doi.org/10.1016/j.ijhydene.2019.11.102

**Table 3 – Calculated values of the surface energy for Fe (100) and VC (100).**

| | $\gamma_{surf}$ [J m$^{-2}$] | |
|---|---|---|
| | Present work | Literature |
| Fe-Relaxed | 2.49 | 2.25 [64]; 2.29 [63] |
| Fe-Unrelaxed | 2.51 | 2.26 [64]; 2.32 [63] |
| VC-Relaxed | 1.25 | 1.27 [55] |
| VC-Unrelaxed | 1.63 | |

changed. The same procedure is adopted for the generation of the Fe surface.

As already mentioned for the Fe-VC interface, all the calculations of the Fe and VC slabs, including those containing H, were done using the parameters shown in Table 1.

### Energetics

*Formation enthalpy*

The formation enthalpy of VC, $H_f$[VC], is calculated as the energy difference between the total energy of bulk VC and the sum of that of its composing elements [46,56,57]:

$$H_f[V_yC_x] = \frac{E[V_yC_x] - yE[V] - xE[C]}{y+x} \quad (2)$$

where $E[V_yC_x]$ is the total energy of $V_yC_x$, and $E$[V] and $E$[C] are the total energies per atom of bulk V and C, respectively. In the present work, a value of $H_f$[VC] = −0.435 eV/atom was obtained, which is consistent with other theoretical values available in the literature [57–60]. The negative value indicates that the formation of bulk VC is energetically favourable with respect to the pure elements. Note that at zero pressure and temperature the total energy and enthalpy are equivalent.

*Surface energies*

In the case of the VC and Fe surfaces, the surface energies [61] were calculated using two different methods [62]: the first one (unrelaxed) consists in calculating the total energy of the system while keeping the atoms fixed in their ideal bulk positions; the second one (relaxed), allows the atoms to move – except for the atoms in the centre of the slab – in order to find their most energetically favourable positions. The dimensions of the simulation box are kept fixed in both cases. The relation used for the calculation of the surface energy of Fe, $\gamma_{Fe-surf}$ is [63].

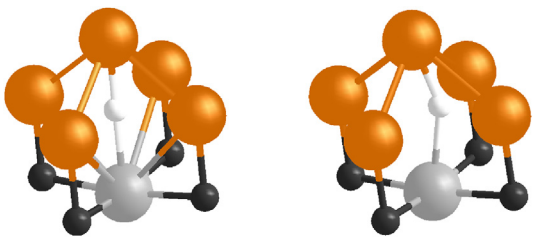

**Fig. 2 – Detail of the octahedral (left) and tetrahedral (right) positions of H in the Fe-VC interface. Fe is drawn in orange, V in grey, C in black and H in white. (For interpretation of the references to colour in this figure legend, the reader is referred to the Web version of this article.)**

$$\gamma_{Fe-surf} = \frac{E^N_{Fe-slab} - NE_{Fe-bulk}}{2A_{Fe-slab}} \quad (3)$$

where $E^N_{Fe-slab}$ is the total energy of a slab of N Fe atoms, $E_{Fe-bulk}$ the total energy of an Fe atom in the bulk, and $A_{Fe-slab}$ is the area of the surface. For the surface energy of VC, $\gamma_{VC-surf}$, the following equation is used:

$$\gamma_{VC-surf} = \frac{E^N_{VC-slab} - NE_{VC-bulk}}{2A_{VC-slab}} \quad (4)$$

where $E^N_{VC-slab}$ is the total energy of a slab containing $N$ VC atom pairs, $E_{VC-bulk}$ is the total energy per VC atom pair of the material in the bulk and $A_{VC-slab}$ is the area of the surface.

The calculated surface energies for the relaxed and unrelaxed cases of VC and Fe are presented in Table 3. The results show that the relaxed surface energies are lower than those for the unrelaxed surfaces. In both cases a good agreement was found with other reported data [55,63,64].

*Interfacial energy*

The energy of the interface is calculated using the following equation [53]:

$$\gamma_{Fe-VC} = \frac{E_{Fe-VC} - nE_{Fe-bulk} - mE_{VC-bulk}}{2A_{Fe-VC}} \quad (5)$$

where $E_{Fe-VC}$ is the total energy of the interface system, $E_{Fe-bulk}$ the total energy per Fe atom in the bulk, $E_{VC-bulk}$ is the total energy per VC atom pair in the bulk, m (n) is the number of Fe atoms (VC atom pairs) in the interface system and $A_{Fe-VC}$ is the area of the interface.

For the interface under consideration the interface energy ($\gamma_{Fe-VC}$) is − 0.090 J m$^{-2}$, comparable to the values of −0.076J m$^{-2}$ and −0.120 J m$^{-2}$ found in the literature [42,54]. The negative value indicates that there is a relatively strong bonding between VC and Fe, and that the formation of the interface is energetically favourable compared to the two separate bulk states [42,53].

## H interaction with the interface

### Solubility

The solubility of H in a given system can be characterised by the dissolution energy $\Delta E_S$, which is defined as [65,66]:

$$\Delta E_S = E_{System+H} - E_{System} - \frac{E[H_2]}{2} \quad (6)$$

where $E_{System}$ is the total energy of a given system, $E_{System+H}$ is the total energy of the same system but containing one interstitial H atom, and $E[H_2]$ is the energy of an $H_2$ molecule in vacuum.

Calculations of the dissolution energy were performed first for H present in the octahedral and tetrahedral position of a Fe cubic supercell containing 16 atoms. Calculations were also done for H in two different positions in the Fe-VC interface plane, corresponding to sites with similar symmetry to the octahedral and terahedral sites in Fe bulk, but with one of the vertices substituted with a V atom (see Fig. 2). In all cases, a

Please cite this article as: Echeverri Restrepo S et al., Density functional theory calculations of iron - vanadium carbide interfaces and the effect of hydrogen, International Journal of Hydrogen Energy, https://doi.org/10.1016/j.ijhydene.2019.11.102

**Table 4 – Dissolution energies ($\Delta E_S$) for a single hydrogen particle in different systems. The calculation of the dissolution energy is performed using Equation (6).**

| Dissolution energy [eV] | | |
|---|---|---|
| | Present work | Literature |
| $Fe_{Octahedral}$ | 0.303 | 0.32 [66]; 0.34 [69] 0.36 [70]; 0.36 [71] |
| $Fe_{Tetrahedral}$ | 0.173 | 0.16 [14]; 0.19 [71] 0.20 [66]; 0.22 [70] 0.25 [65] |
| $Fe-VC_{Octahedral}$ | 0.097 | |
| $Fe-VC_{Tetrahedral}$ | 0.067 | |
| $Fe-VC_{C-Vacancy-interface}$ | −0.382 | |
| $Fe-VC_{C-Vacancy-bulk}$ | −0.410 | |

structural relaxation of the atomic positions and of the lattice vectors is carried out. The resulting dissolution energies are presented in Table 4.

In the case of bcc Fe, the calculated dissolution energies are consistent with those from other calculations, see Table 4. The dissolution energy for the tetrahedral site is lower than that for the octahedral site, meaning that H atoms will have the tendency to occupy the tetrahedral site. Indirect experimental evidence also favours tetrahedral occupancy [67].

A similar trend is found when comparing the octahedral and tetrahedral sites in the interface. The lower energy of the tetrahedral site shows that H will preferably segregate towards this site. Also, the lower dissolution energies of H at the interface indicate that the interfacial regions are more favourable for H than the bulk interstitial sites, and that it will have the tendency to segregate towards the interface.

In addition to the perfect interfaces, the segregation of H at C vacancies in the vicinity of the interface was also investigated. Two configurations were considered: in the first one, a C atom from the interface plane was removed; in the second one, the second closest C atom from the interface was removed (which will be referred to as 'vacancy in bulk VC'). It was found that these two configurations have the lowest dissolution energies among the analysed sites, making them the strongest trapping sites for H (see Table 4).

We compare our results with similar calculations from the literature but for a system containing an interface between Fe and TiC [14] (instead of VC). We see that, qualitatively, the trends are the same: the deepest trap for a H atom is a C vacancy in the bulk of the precipitate, followed by a vacancy at the interface. This is consistent with experimental findings that substoichiometric TiC allows the insertion of atomic H [68]. Similar to our results with VC, they also conclude that, at the interface, the tetrahedral position is more stable than the octahedral one.

### *Trap escape energy*

Recent characterisation work [13] of a vanadium-carbide precipitation-steel using Atom Probe Tomograpy (APT) and hydrogen Thermal Desorption Spectroscopy (TDS) analysis found that there are two possible types of H traps resulting from the presence of VC precipitates in steels. The deeper trapping energy was estimated to be 59.6±10.0 kJmol$^{-1}$ (0.618±0.100 eV) and was attributed to the interface carbon vacancy. The shallower trapping energy was estimated to be 24.8±5.0 kJmol$^{-1}$ (0.257 ±0.050 eV) but its origin could not be clearly determined. And independent analysis of the same experiments using the generalised Kissinger equation gives values of 42.6±0.7 kJmol$^{-1}$(0.442±0.007 eV) for the deep traps and of 23.5±1.2 kJmol$^{-1}$ (0.244±0.012 eV) for the shallow ones [72].

To compare our results with the experiments, we follow the method proposed in Ref. [14]. We calculate the trap escape energy ($\Delta E_E$), which is the energy needed for H to escape from a given trap to bulk Fe:

$$\Delta E_E = -(\Delta E_S - \Delta E_S[Fe_{Tetrahedral}]) + \Delta E_{mig} \quad (7)$$

where $\Delta E_{mig}$ is the energy barrier for H migration in Fe and is considered to be equal to its bulk value of 0.09 eV [73]. Note that this equation is valid for H at the interface or in a C vacancy at the interface, but not for H trapped in a vacancy in bulk. For the latter case, it would be necessary to include the segregation and migration energies of H in bulk VC.

We calculate the trap escape energy for H in a C vacancy at the interface ($\Delta E_E[Fe-VC_{C-Vacancy-interface}]$) and in the tetrahedral position at the perfect interface ($\Delta E_E[Fe-VC_{Tetrahedral}]$). We obtain values of 0.645 eV and 0.196 eV, respectively.

The calculated value of $\Delta E_E[Fe-VC_{C-Vacancy-interface}]$ agrees with the experimentally measured deeper trapping energy (0.645 eV vs 0.618 ±0.1 eV), which was also attributed to the interface carbon vacancy [13].

Our calculated value of $\Delta E_E[Fe-VC_{Tetrahedral}]$ is akin to the shallower trap that was found experimentally (0.196 eV vs 0.257 ±0.05 eV). This leads us to suggest that the shallower trap, whose origin is still debated in the literature, comes from the H trapped at the coherent boundary.

### *Crack formation*

In order to check if the presence of H in the interface facilitates the formation of a crack along it –and, thus, the embrittlement of the material–, the work of separation [74,75] of the interface with and without H are considered. The work of separation can be interpreted as the excess energy needed for the separation of the two grains along the interface and it corresponds to the energy difference between the fractured surfaces and the interface. In this sense, a change in the work of separation represents a change in the brittleness of the interface. Here it is important to note that, especially in ductile materials, the mechanical work needed to separate an interface can be larger than its work of separation [76].

In the case of the pristine Fe-VC interface, the work of separation $\mathscr{W}_{Fe-VC}$ is given by

$$\mathscr{W}_{Fe-VC} = \gamma_{VC-surf} + \gamma_{Fe-surf} - \gamma_{Fe-VC} \quad (8)$$

where $\gamma_{VC-surf}$ and $\gamma_{Fe-surf}$ are the surface energies of VC and Fe respectively and $\gamma_{Fe-VC}$ is the energy of a VC-Fe interface.

In the case of the H containing interface, the system with the H atom in the tetrahedral site is considered (see Fig. 2) due to its lower dissolution energy. For the behaviour of H after the separation of the interface, two cases are considered: in the first one, it is assumed that after fracture the H atom stays

Please cite this article as: Echeverri Restrepo S et al., Density functional theory calculations of iron - vanadium carbide interfaces and the effect of hydrogen, International Journal of Hydrogen Energy, https://doi.org/10.1016/j.ijhydene.2019.11.102

attached to the Fe surface (after relaxation the H atom moves from the tetrahedral to the more energetically stable octahedral position on the surface). In this case the work of separation is given by

$$\mathscr{W}_{(Fe+H)-VC} = \gamma_{VC-surf} + \gamma_{Fe-surf+H} - \gamma_{Fe-VC+H} \quad (9)$$

where, $\gamma_{Fe-surf+H}$ is the energy of a Fe slab with an H atom on the surface and $\gamma_{Fe-VC-H}$ is the energy of a VC-Fe interface with an H atom in the tetrahedral position.

In the second case, it is assumed that once the two free surfaces are formed, H detaches from the Fe surface. The work of separation $\mathscr{W}_{Fe-VC-H}$ is then given by

$$\mathscr{W}_{Fe-VC-H} = \gamma_{VC-surf} + \gamma_{Fe-surf} + \frac{E[H_2]}{2A_{Fe-VC}} - \gamma_{Fe-VC+H} \quad (10)$$

where $E[H_2]$ is the energy of an $H_2$ molecule in vacuum and $A_{Fe-VC}$ is the area of the interface.

The resultant values of the work of separation are 3.83 J m$^{-2}$, 3.93 J m$^{-2}$ and 3.74 J m$^{-2}$ for $\mathscr{W}_{Fe-VC}$, $\mathscr{W}_{(Fe+H)-VC}$ and $\mathscr{W}_{Fe-VC-H}$, respectively. Note that although in the case of $\mathscr{W}_{(Fe+H)-VC}$ there is a slight decrease in the work of separation, even with the most pessimistic assumption its reduction is around 2%; this value is negligible considering the high concentration of H that was used in the calculations.

## Conclusions

In the present work, a density functional theory study of H interaction with perfect and defective (100)Fe/(100)VC interfaces was carried out. The calculations show that the perfect coherent interface traps H only weakly, but much stronger trapping can be expected at C vacancies, both at the interface and in VC bulk. Thermodynamic estimates based on the work of separation show a negligible influence of H on the interface strength but more elaborate treatment is necessary for a more reliable prediction. The presented theoretical results are consistent with those obtained for other carbides, in particular with titanium carbide (TiC) [14], and with experimental findings. Nevertheless, more work is still needed to fully resolve the positive role of carbide precipitates on the improved resistance of steels to hydrogen embrittlement [2].

## Acknowledgments

SER would like to thank Mohamed Sherif from SKF Research & Technology Development (RTD), SKF B.V., Houten, The Netherlands and Robin Chaudret from Scienomics, Paris, France for useful discussions. This work was supported in part through the computational resources and staff contributions provided for the Comlab high performance computing facility at SKF Research & Technology Development, Houten, The Netherlands.

MM gratefully acknowledges the financial support under the scope of the COMET program within the K2 Center "Integrated Computational Material, Process and Product Engineering (IC-MPPE)" (Project No 859480). This program is supported by the Austrian Federal Ministries for Transport, Innovation and Technology (BMVIT) and for Digital and Economic Affairs (BMDW), represented by the Austrian research funding association (FFG), and the federal states of Styria, Upper Austria and Tyrol. ATP is supported by EPSRC under the HEmS Programme Grant EP/L014742.

The present results have been obtained through the use of the ABINIT code, a common project of the Université Catholique de Louvain, Corning Incorporated, and other contributors. The images were generated using the software V_Sim (http://inac.cea.fr/L_Sim/V_Sim/).

## REFERENCES

[1] Bhadeshia H. Prog Mater Sci 2012;57:268–435. URL, http://linkinghub.elsevier.com/retrieve/pii/S0079642511000922. 10.1016/j.pmatsci.2011.06.002.
[2] Szost B, Vegter R, Rivera-Díaz-del Castillo P. Mater Des 2013;43:499–506. URL, http://linkinghub.elsevier.com/retrieve/pii/S0261306912004827. 10.1016/j.matdes.2012.07.030.
[3] Evans M-H, Richardson A, Wang L, Wood R. Wear 2013;306:226–41. URL, http://linkinghub.elsevier.com/retrieve/pii/S0043164813001877. 10.1016/j.wear.2013.03.008.
[4] Vegter RH, Slycke JT, Beswick J, Dean SW. J ASTM Int 2010;7:102543. URL, http://www.astm.org/doiLink.cgi?JAI102543. 10.1520/JAI102543.
[5] Sofronis P. AIP Conf Proc 2006;837:64–70. URL, http://scitation.aip.org/content/aip/proceeding/aipcp/10.1063/1.2213060. 10.1063/1.2213060.
[6] Szost B, Rivera-Díaz-del Castillo P. Scripta Materialia 2013;68:467–70. URL, http://linkinghub.elsevier.com/retrieve/pii/S1359646212007385. 10.1016/j.scriptamat.2012.11.018.
[7] Birnbaum H, Sofronis P. Mater Sci Eng A 1994;176:191–202. https://doi.org/10.1016/0921-5093(94)90975-X.
[8] Szost BA, Vegter RH, Rivera-Díaz-del Castillo PEJ. Metall Mater Trans A 2013;44:4542–50. URL, http://link.springer.com/10.1007/s11661-013-1795-7. doi:10.1007/s11661-013-1795-7.
[9] Hohenberg P, Kohn W. Phys Rev 1964;136:B864–71. https://doi.org/10.1103/PhysRev.136.B864. URL, http://link.aps.org/doi/10.1103/PhysRev.136.B864.
[10] Kohn W, Sham LJ. Phys Rev 1965;140:A1133–8. https://doi.org/10.1103/PhysRev.140.A1133. URL, http://link.aps.org/doi/10.1103/PhysRev.140.A1133.
[11] Takahashi J, Kawakami K, Tarui T. Scripta Materialia 2012;67:213–6. https://doi.org/10.1016/j.scriptamat.2012.04.022. URL, http://linkinghub.elsevier.com/retrieve/pii/S1359646212002631.
[12] Chen Y-S, Haley D, Gerstl SSA, London AJ, Sweeney F, Wepf RA, Rainforth WM, Bagot PAJ, Moody MP. Science 2017;355:1196–9. URL, http://www.sciencemag.org/lookup/doi/10.1126/science.aal2418. 10.1126/science.aal2418.
[13] Takahashi J, Kawakami K, Kobayashi Y. Acta Mater 2018;153:193–204. URL, https://linkinghub.elsevier.com/retrieve/pii/S1359645418303549. 10.1016/j.actamat.2018.05.003.
[14] Di Stefano D, Nazarov R, Hickel T, Neugebauer J, Mrovec M, Elsässer C. Phys Rev B 2016;93:184108. URL, https://link.aps.org/doi/10.1103/PhysRevB.93.184108. 10.1103/PhysRevB.93.184108.
[15] Gonze X, Amadon B, Anglade PM, Beuken JM, Bottin F, Boulanger P, Bruneval F, Caliste D, Caracas R, Côté M,

Deutsch T, Genovese L, Ghosez P, Giantomassi M, Goedecker S, Hamann DR, Hermet P, Jollet F, Jomard G, Leroux S, Mancini M, Mazevet S, Oliveira MJT, Onida G, Pouillon Y, Rangel T, Rignanese GM, Sangalli D, Shaltaf R, Torrent M, Verstraete MJ, Zerah G, Zwanziger JW. Comput Phys Commun 2009;180:2582–615. https://doi.org/10.1016/j.cpc.2009.07.007. 10.1016/j.cpc.2009.07.007.

[16] Becke AD. Phys Rev A 1988;38:3098–100. URL, http://link.aps.org/doi/10.1103/PhysRevA.38.3098. 10.1103/PhysRevA.38.3098. arXiv:PhysRevA.38.3098.

[17] Langreth DC, Mehl MJ. Phys Rev B 1983;28:1809–34. https://doi.org/10.1103/PhysRevB.28.1809.

[18] Perdew JP, Chevary JA, Vosko SH, Jackson KA, Pederson MR, Singh DJ, Fiolhais C. Phys Rev B 1992;46:6671–87. URL, http://link.aps.org/doi/10.1103/PhysRevB.46.6671. 10.1103/PhysRevB.46.6671.

[19] Perdew JP, Chevary JA, Vosko SH, Jackson KA, Pederson MR, Singh DJ, Fiolhais C. Phys Rev B 1993;48. 4978–4978. URL, http://link.aps.org/doi/10.1103/PhysRevB.48.4978.2. 10.1103/PhysRevB.48.4978.2.

[20] Perdew JP, Burke K, Ernzerhof M. Phys Rev Lett 1996;77:3865–8. URL: http://www.ncbi.nlm.nih.gov/pubmed/10062328{\%}5Cnhttp://link.aps.org/doi/10.1103/PhysRevLett.77.3865{\%}5Cnhttp://link.aps.org/abstract/PRL/v77/p3865Ωhttps://link.aps.org/doi/10.1103/PhysRevLett.77.3865. doi:10.1103/PhysRevLett.77.3865.

[21] Torrent M, Jollet F, Bottin F, Zérah G, Gonze X. Comput Mater Sci 2008;42:337–51. https://doi.org/10.1016/j.commatsci.2007.07.020.

[22] Blöchl PE. Phys Rev B 1994;50:17953–79. URL, http://link.aps.org/doi/10.1103/PhysRevB.50.17953. 10.1103/PhysRevB.50.17953.

[23] Garrity KF, Bennett JW, Rabe KM, Vanderbilt D. Comput Mater Sci 2014;81:446–52. URL, http://linkinghub.elsevier.com/retrieve/pii/S0927025613005077. 10.1016/j.commatsci.2013.08.053.

[24] Kolos W, Roothaan CCJ. Rev Mod Phys 1960;32:219–32. URL, http://link.aps.org/doi/10.1103/RevModPhys.32.219. 10.1103/RevModPhys.32.219.

[25] Liu Y, Huang S, Ding J, Yang Y, Zhao J. Int J Hydrogen Energy 2019;44:6093–102. URL, https://linkinghub.elsevier.com/retrieve/pii/S0360319919301235. 10.1016/j.ijhydene.2019.01.049.

[26] Srivastava A, Chauhan M, Singh R. Phase Transitions 2011;84:58–66. URL, http://www.tandfonline.com/doi/abs/10.1080/01411594.2010.509644. 10.1080/01411594.2010.509644.

[27] Hao A-M, Zhou T-J, Zhu Y, Zhang X-Y, Liu R-P. Chinese Phys B 2011;20:047103. URL, http://stacks.iop.org/1674-1056/20/i=4/a=047103?key=crossref.cfbbf50bcffeb32f8556cf4f4184aac0. 10.1088/1674-1056/20/4/047103.

[28] Nakamura K, Yashima M. Mater Sci Eng B 2008;148:69–72. URL, http://linkinghub.elsevier.com/retrieve/pii/S092151070700503X. 10.1016/j.mseb.2007.09.040.

[29] Zhukov V, Gubanov V. J Phys Chem Solids 1987;48:187–95. URL, http://linkinghub.elsevier.com/retrieve/pii/0022369787900837. 10.1016/0022-3697(87)90083-7.

[30] Vojvodic A, Ruberto C. J Phys Condens Matter: Inst Phys J 2010;22:375501. URL, http://www.ncbi.nlm.nih.gov/pubmed/21403197. 10.1088/0953-8984/22/37/375501.

[31] Sun Z, Ahuja R, Lowther J. Solid State Commun 2010;150:697–700. URL, http://linkinghub.elsevier.com/retrieve/pii/S0038109810000803. 10.1016/j.ssc.2010.01.043.

[32] Liu H, Zhu J, Liu Y, Lai Z. Mater Lett 2008;62:3084–6. URL, http://linkinghub.elsevier.com/retrieve/pii/S0167577X08001602. 10.1016/j.matlet.2008.01.136.

[33] Wolf W, Podloucky R, Antretter T. Philos Mag B 1999;79:839–58. URL, http://journalsonline.tandf.co.uk/Index/10.1080/014186399256943. 10.1080/014186399256943.

[34] Tran F, Laskowski R, Blaha P, Schwarz K. Phys Rev B Condens Matter Mater Phys 2007;75:1–14. https://doi.org/10.1103/PhysRevB.75.115131.

[35] Zhang LQ, Cheng Y, Niu ZW. J At Mol Sci 2014;5:81–94. URL, http://www.global-sci.org/jams/volumes/v5n1/pdf/051-81.pdf. 10.4208/jams.072513.101413a.

[36] Finnis MW, Sinclair JE. Philos Mag A 1984;50:45–55. URL, http://www.tandfonline.com/doi/abs/10.1080/01418618408244210. 10.1080/01418618408244210.

[37] Koči L, Ma Y, Oganov AR, Souvatzis P, Ahuja R. Phys Rev B 2008;77:214101. URL, http://link.aps.org/doi/10.1103/PhysRevB.77.214101. 10.1103/PhysRevB.77.214101.

[38] Hasegawa M, Nishidate K. Phys Rev B 2004;70:205431. URL, http://link.aps.org/doi/10.1103/PhysRevB.70.205431. 10.1103/PhysRevB.70.205431.

[39] Rydberg H, Jacobson N, Hyldgaard P, Simak S, Lundqvist B, Langreth D. Surface science, vols. 532–535; 2003. p. 606–10. URL, http://linkinghub.elsevier.com/retrieve/pii/S0039602803001092. 10.1016/S0039-6028(03)00109-2.

[40] Baskin Y, Meyer L. Phys Rev 1955;100. 544–544. URL, http://link.aps.org/doi/10.1103/PhysRev.100.544. 10.1103/PhysRev.100.544.

[41] Haas P, Tran F, Blaha P. Phys Rev B - Condens Matter Mater Phys 2009;79:1–10. https://doi.org/10.1103/PhysRevB.79.085104.

[42] Fors DHR, Wahnström G. Phys Rev B 2010;82:195410. URL, http://link.aps.org/doi/10.1103/PhysRevB.82.195410. 10.1103/PhysRevB.82.195410.

[43] Hung A, Yarovsky I, Muscat J, Russo S, Snook I, Watts R. Surface Sci 2002;501:261–9. URL, http://linkinghub.elsevier.com/retrieve/pii/S0039602801017629. 10.1016/S0039-6028(01)01762-9.

[44] Davey WP. Phys Rev 1925;25:753–61. https://doi.org/10.1103/PhysRev.25.753.

[45] Ridley N, Stuart H. J Phys D: Appl Phys 2002;1:1291–5. https://doi.org/10.1088/0022-3727/1/10/308.

[46] Jang JH, Lee CH, Heo YU, Suh DW. Acta Materialia 2012;60:208–17. https://doi.org/10.1016/j.actamat.2011.09.051. 10.1016/j.actamat.2011.09.051.

[47] Epicier T, Acevedo D, Perez M. Philos Mag 2008;88:31–45. URL, http://www.tandfonline.com/doi/abs/10.1080/14786430701753816. 10.1080/14786430701753816.

[48] Wei F-G, Hara T, Tsuzaki K. In: Advanced steels. Berlin, Heidelberg: Springer Berlin Heidelberg; 2011. p. 87–92. https://doi.org/10.1007/978-3-642-17665-4_11. URL, http://link.springer.com/10.1007/978-3-642-17665-4.

[49] Randle V. The measurement of grain boundary geometry, Electron microscopy in materials science series. Inst Phys 1993. URL: http://books.google.nl/books?id=mgprQgAACAAJ.

[50] Echeverri Restrepo S, Tamayo Giraldo S, Thijsse BJ. Model Simul Mater Sci Eng 2013;21:055017. URL: http://stacks.iop.org/0965-0393/21/i=5/a=055017?key=crossref.060fedf363c00b209f02970a28b12955. 10.1088/0965-0393/21/5/055017.

[51] Echeverri Restrepo S, Thijsse BJ. MRS Proceedings 2011;1224. 1224–GG05–03. URL: https://doi.org/10.1557/PROC-1224-GG05-03Ωhttp://journals.cambridge.org/abstract{_}S1946427400019849Ωhttp://www.journals.cambridge.org/abstract{_}S1946427400019849. doi:10.1557/PROC-1224-GG05-03.

[52] Kawakami K, Matsumiya T. ISIJ Int 2012;52:1693–7. URL: http://jlc.jst.go.jp/DN/JST.JSTAGE/isijinternational/52.1693?lang=en{\&}from=CrossRef{\&}type=abstract. doi:10.2355/isijinternational.52.1693.

[53] Park N-Y, Choi J-H, Cha P-R, Jung W-S, Chung S-H, Lee S-C. J Phys Chem C 2013;117:187–93. URL, http://pubs.acs.org/doi/abs/10.1021/jp306859n. 10.1021/jp306859n.

[54] Chung S-H, Ha H-P, Jung W-S, Byun J-Y. ISIJ Int 2006;46:1523–31. URL, http://joi.jlc.jst.go.jp/JST.JSTAGE/isijinternational/46.1523?from=CrossRef. 10.2355/isijinternational.46.1523.

Please cite this article as: Echeverri Restrepo S et al., Density functional theory calculations of iron - vanadium carbide interfaces and the effect of hydrogen, International Journal of Hydrogen Energy, https://doi.org/10.1016/j.ijhydene.2019.11.102

[55] Siegel DJ, Hector LG, Adams JB. Acta Materialia 2002;50:619–31. URL, http://linkinghub.elsevier.com/retrieve/pii/S1359645401003615. 10.1016/S1359-6454(01)00361-5.
[56] Ande CK, Sluiter MHF. Metall Mater Trans A 2012;43:4436–44. URL, http://link.springer.com/10.1007/s11661-012-1229-y. 10.1007/s11661-012-1229-y.
[57] Chong X, Jiang Y, Zhou R, Feng J. RSC Adv 2014;4:44959–71. URL, http://xlink.rsc.org/?DOI=C4RA07543A. 10.1039/C4RA07543A.
[58] Ozoliņš V, Häglund J. Phys Rev B 1993;48:5069–76. URL, http://link.aps.org/doi/10.1103/PhysRevB.48.5069. 10.1103/PhysRevB.48.5069.
[59] Limmer KR. First-principles investigations of iron-based alloys and their properties. Ph.D. thesis. Missouri University of Science and Technology; 2014. URL, http://scholarsmine.mst.edu/doctoral_dissertations/2347.
[60] Wang B, Liu Y, Ye J. Physica Scripta 2013;88:015301. URL, http://stacks.iop.org/1402-4896/88/i=1/a=015301?key=crossref.b126b0c89b1d6df7344e4b34e339d659. 10.1088/0031-8949/88/01/015301.
[61] Wang JW, Gong H. Int J Hydrogen Energy 2014;39:6068–75. URL, https://linkinghub.elsevier.com/retrieve/pii/S0360319914002067. 10.1016/j.ijhydene.2014.01.126.
[62] Marlo M, Milman V. Phys Rev B 2000;62:2899–907. URL, http://link.aps.org/doi/10.1103/PhysRevB.62.2899. 10.1103/PhysRevB.62.2899.
[63] Spencer MJS, Hung A, Snook IK, Yarovsky I. Surface Sci 2002;513:389–98. https://doi.org/10.1016/S0039-6028(02)01809-5.
[64] Błoński P, Kiejna A. Vacuum 2004;74:179–83. URL, http://linkinghub.elsevier.com/retrieve/pii/S0042207X04000132. 10.1016/j.vacuum.2003.12.118.
[65] Du YA, Ismer L, Rogal J, Hickel T, Neugebauer J, Drautz R. Phys Rev B 2011;84:144121. URL, http://link.aps.org/doi/10.1103/PhysRevB.84.144121. 10.1103/PhysRevB.84.144121.
[66] Jiang DE, Carter EA. Phys Rev B 2004;70:064102. URL, http://link.aps.org/doi/10.1103/PhysRevB.70.064102. 10.1103/PhysRevB.70.064102.
[67] Hirth JP. Metall Trans A 1980;11:861–90. URL, http://link.springer.com/10.1007/BF02654700. 10.1007/BF02654700.
[68] Nguyen J, Glandut N, Jaoul C, Lefort P. Int J Hydrogen Energy 2015;40:8562–70. URL, https://linkinghub.elsevier.com/retrieve/pii/S0360319915011271. doi:10.1016/j.ijhydene.2015.05.009.
[69] Song EJ, Bhadeshia H, Suh D-W. Corros Sci 2013;77:379–84. URL, https://linkinghub.elsevier.com/retrieve/pii/S0010938X13003533. 10.1016/j.corsci.2013.07.043.
[70] Ramasubramaniam A, Itakura M, Ortiz M, Carter E. J Mater Res 2008;23:2757–73. URL, http://www.journals.cambridge.org/abstract_S0884291400030259. 10.1557/JMR.2008.0340.
[71] Miwa K, Fukumoto A. Phys Rev B 2002;65:155114. URL, http://link.aps.org/doi/10.1103/PhysRevB.65.155114. 10.1103/PhysRevB.65.155114.
[72] Kirchheim R. Scripta Materialia 2019;160:62–5. URL, https://linkinghub.elsevier.com/retrieve/pii/S1359646218305943. 10.1016/j.scriptamat.2018.09.043.
[73] Di Stefano D, Mrovec M, Elsässer C. Phys Rev B 2015;92:224301. URL, http://link.aps.org/doi/10.1103/PhysRevB.92.224301. 10.1103/PhysRevB.92.224301.
[74] Lozovoi AY, Paxton AT, Finnis MW. Phys Rev B 2006;74:155416. URL, http://link.aps.org/doi/10.1103/PhysRevB.74.155416. 10.1103/PhysRevB.74.155416. arXiv:0608508.
[75] Finnis MW. J Phys: Condens Matter 1996;8:5811–36. URL, http://stacks.iop.org/0953-8984/8/i=32/a=003?key=crossref.6b2d897a5a15cc01a9a7a0826bfa6dab. 10.1088/0953-8984/8/32/003.
[76] Liu LM, Wang SQ, Ye HQ. J Phys: Condens Matter 2005;17:5335–48. URL, http://iopscience.iop.org/0953-8984/17/35/002. 10.1088/0953-8984/17/35/002.

Please cite this article as: Echeverri Restrepo S et al., Density functional theory calculations of iron - vanadium carbide interfaces and the effect of hydrogen, International Journal of Hydrogen Energy, https://doi.org/10.1016/j.ijhydene.2019.11.102